fermentation

MDPI

Article

Comparative Transcriptomic Responses Directed Towards Reporter Metabolic Routes of *Mucor circinelloides* WJ11 for Growth Adaptation and Lipid Overproduction

Fanyue Li [1,2,†], Nang Myint Phyu Sin Htwe [3,†], Preecha Patumcharoenpol [1], Junhuan Yang [4], Kobkul Laoteng [5], Yuanda Song [2,6,*] and Wanwipa Vongsangnak [7,8,*]

1 Interdisciplinary Graduate Programs in Bioscience, Faculty of Science, Kasetsart University, Bangkok 10900, Thailand; lfyue@sdut.edu.cn (F.L.); preecha.pa@ku.th (P.P.)
2 Colin Ratledge Center for Microbial Lipids, School of Agricultural Engineering and Food Science, Shandong University of Technology, 266 Xincun West Road, Zibo 255000, China
3 Kasetsart University International College, Kasetsart University, Bangkok 10900, Thailand; nangmyintphyusin.h@ku.th
4 Department of Food Sciences, College of Food Science and Engineering, Lingnan Normal University, Zhanjiang 524048, China; yangjh@lingnan.edu.cn
5 Industrial Bioprocess Technology Research Team, Functional Ingredients and Food Innovation Research Group, National Center for Genetic Engineering and Biotechnology (BIOTEC), National Science and Technology Development Agency (NSTDA), Pathum Thani 12120, Thailand; kobkul@biotec.or.th
6 School of Basic Medicine, Qilu Medical University, Zibo 255300, China
7 Department of Zoology, Faculty of Science, Kasetsart University, Bangkok 10900, Thailand
8 Omics Center for Agriculture, Bioresources, Food, and Health, Kasetsart University, Bangkok 10900, Thailand
* Correspondence: ysong@sdut.edu.cn (Y.S.); wanwipa.v@ku.ac.th (W.V.)
† These authors contributed equally to this work.

Abstract: Research into the cellular metabolic adaptations of *Mucor circinelloides* has gained significant interest due to its capability for lipid production, which has critical industrial applications. To address the regulatory mechanisms at the systems level, this study aimed to explore the global metabolic responses associated with lipid production in high and low lipid-producing strains of *M. circinelloides*, WJ11 and CBS277.49, respectively, through comparative transcriptome analysis and genome-scale model-driven analysis. The transcriptome analysis of expressed genes in *M. circinelloides* WJ11 (6398 genes), and CBS277.49 (6008 genes) were analyzed and compared. The results revealed 2811 significantly differentially expressed genes and highlighted strain-dependent differences in growth behavior and lipid production of *M. circinelloides* at the fast-growing stage, driven by transcriptional regulation across key metabolic pathways. Through genome-scale model-driven analysis, we identified 20 significant reporter metabolites that provide insights into the mechanisms employed by the WJ11 strain to optimize growth for lipid production in the subsequent lipid-accumulating stage. These interplay mechanisms are primarily involved in glycolysis, the TCA cycle, leucine metabolism, energy metabolism, and one-carbon metabolism towards lipid metabolism. These findings provide valuable insights into the regulatory mechanisms underlying lipid production in *Mucor* and highlight potential pathways for genetic and physiological optimization in high lipid-producing strains like WJ11. This research advances our understanding of how metabolic networks are interconnected and how they can be leveraged for more efficient lipid overproduction.

Keywords: genome-scale analysis; lipid metabolism; microbial lipids; *Mucor circinelloides*; transcriptome

Academic Editors: Frank Vriesekoop and Penka Petrova

Received: 31 December 2024
Revised: 18 January 2025
Accepted: 26 January 2025
Published: 1 February 2025

Citation: Li, F.; Htwe, N.M.P.S.; Patumcharoenpol, P.; Yang, J.; Laoteng, K.; Song, Y.; Vongsangnak, W. Comparative Transcriptomic Responses Directed Towards Reporter Metabolic Routes of *Mucor circinelloides* WJ11 for Growth Adaptation and Lipid Overproduction. *Fermentation* **2025**, *11*, 61. https://doi.org/10.3390/fermentation11020061

1. Introduction

Long-chain unsaturated fatty acids are essential for maintaining human health, yet cannot be synthesized by the body [1,2]. Traditionally, these essential fatty acids have been sourced from plants and animals, but the intake ratios are often unbalanced, which can limit their health benefits [3]. Studies suggest that a more beneficial ratio of polyunsaturated fatty acids (PUFAs), especially linolenic acid to linoleic acid, ranges from 1:1 to 1:4 [4–6]. These beneficial PUFAs are recognized for their anti-inflammatory and analgesic properties [7,8], offering significant health advantages. While evening primrose oil has historically been a primary source of PUFAs, its low yield and high production costs [9] have prompted researchers to seek more efficient alternatives.

Oil production from filamentous fungi presents several advantages, including a short production cycle, independence from seasonal fluctuations and arable land, and the absence of heavy metals and pesticide residues [10,11]. Moreover, the oils produced by fungi closely resemble those found in plants, making them sustainable alternatives [12,13]. Among filamentous fungi, *Mucor circinelloides* and other *Mucor* species is a well-known oleaginous fungus that accumulates high levels of lipids, particularly under specific culture conditions [14,15]. The main storage form of lipids in *M. circinelloides* is triacylglycerol, mainly found in lipid bodies. Moreover, this fungus is capable of synthesizing γ-linolenic acid (GLA, C18:3 n-6; cis 6, 9, 12-octadecatrienoic acid), a nutritionally important PUFA that has beneficial effects on human and animal health, further highlighting the potential of *M. circinelloides* as a promising source of valuable oils. *M. circinelloides* produces large quantities of enzymes, including amylases, proteases, and lipases (hundreds of tons per year), which are used in various industries [16,17]. These enzymes are marketed under trademarks like Termamyl® (amylase), Optidry® (protease), and Liquozyme® (lipase). In addition, it is also being explored for mycoprotein production as a meat alternative and for the creation of biodegradable plastics like polyhydroxyalkanoates (PHA) for sustainable packaging [18,19].

Investigating high-throughput omics technology is highly needed to improve our understanding of *M. circinelloides*. In previous studies, Tang et al. [20] have reported the genome of a high lipid-producing *M. circinelloides* WJ11 (36% lipid in cell dry weight, DCW) and compared it to that of the low lipid-producing strain, CBS 277.49 (15% *w*/*w* lipid, DCW) [21]. Later, Tang et al. [22] also found changes in protein expression levels in *M. circinelloides* WJ11 under nitrogen deficiency during lipid accumulation. Additionally, the discrimination in lipid contents between *M. circinelloides* WJ11 and CBS277.49 has been documented. Furthermore, 13C-metabolic flux comparisons between these strains revealed key enzymatic reactions participated in supplying the precursors, e.g., acetyl-CoA and NADPH for fatty acid synthesis in WJ11, which had higher fluxes than those of CBS277.49, especially in the lipid accumulation phase [23].

In the context of metabolism, an analysis of genome-scale metabolic networks of the *M. circinelloides* WJ11 and CBS277.49 revealed the integration of targeted genes with the expressed proteins of the fungal cells during the lipid accumulation stage [24]. Recently, the genome-scale metabolic model (GEM) has become a useful computational tool for predicting metabolic behaviors. This model is often used in systems biology alongside other modern technologies, such as gene editing and synthetic biology [25]. More recently, GEMs for *M. circinelloides* strains CBS277.49 [26] and WJ11 [27] have been enhanced by analyzing their growth behavior across various nutrient sources. Very recently, there have been reports on transcriptional regulation, e.g., transcriptional regulator SREBP1, energy regulator AMPK, and regulator AreA for nitrogen metabolism involved in lipid biosynthesis in *M. circinelloides* WJ11 [28–30].

To date, the transcriptional regulation of cellular mechanisms at the systems level has been poorly characterized between the two strains. Therefore, this study aimed to explore the metabolic transcriptome responses of *M. circinelloides* WJ11 and compare them with the CBS 277.49 strain. RNA-Seq data for both strains were obtained and then processed with the MGISEQ-2000RS platform through a comparative transcriptomics analysis. By integrating comparative transcriptome data with proteomics [31], ^{13}C-metabolic flux analysis [23], and genome-scale model-driven analysis, the reporter metabolic routes driving rapid growth and lipid overproduction in *M. circinelloides*, particularly under specific culture conditions in the WJ11 strain were uncovered. This study provides valuable insights into the systems-wide mechanisms of lipid overproduction in *M. circinelloides*, offering useful knowledge for the large-scale production of oleochemicals and specialty lipids.

2. Materials and Methods

2.1. Fungal Strains Cultivations

M. circinelloides strains WJ11 and *M. circinelloides* CBS277.49 were used in this study. For fungal cultivation, inoculum preparation of each strain was performed by growing them in K&R medium, each liter of which consisted of 30.0 g glucose, 1.5 g $MgSO_4 \cdot 7H_2O$, 3.3 g ammonium tartrate, 7.0 g KH_2PO_4, 2.0 g Na_2HPO_4, 1.5 g yeast extract, 0.1 g $CaCl_2 \cdot 2H_2O$, 8.0 mg $FeCl_3 \cdot 6H_2O$, 1 mg $ZnSO_4 \cdot 7H_2O$, 0.1 mg $CuSO_4 \cdot 5H_2O$, 0.1 mg $Co(NO_3)_2 \cdot 6H_2O$, and 0.1 mg $MnSO_4 \cdot 5H_2O$ [32], with shaking at 150 rpm, 28 ± 1 °C. The 24 h culture was then inoculated into a 2.0 L fermenter (BioFlo/CelliGen115, New Brunswick Scientific, NJ, USA) with a 1.5 L working volume of the medium broth containing 80 g/L glucose and 2 g/L ammonium tartrate. The cultivation conditions were constantly controlled, including a culture temperature of 28 ± 1 °C, pH of 6.0, stirring speed of 700 rpm, and an airflow rate of 1 vvm [33].

2.2. Biomass and Lipid Determination

The harvested mycelial samples were dried using a freeze dryer at −30 °C for two days. Dried samples were then weighted and subjected to calculate biomass concentration represented as dry cell weight (DCW). For growth determination, the specific growth rate (μ, h^{-1}) was calculated using experimental data, including biomass concentrations (C_X, g/L) and time intervals (t) according to Formula (1).

$$\mu = \frac{lnC_{X_2} - lnC_{X_1}}{t_2 - t_1} \quad (1)$$

The total lipid of dried mycelia was extracted using a chloroform/methanol (2:1, v/v) solution and then methylated with 4 mol/L methanolic HCl at 60 °C for 3 h. The fatty acid methyl esters were afterward extracted with n-hexane and analyzed with gas chromatography with a flame ionization detector (GC-FID) [34] using a 30 m × 0.32 mm DB-WAXETR column (0.25 μm film thickness) [35]. The GC analysis was operated at 120 °C for 3 min, ramped to 200 °C at 5 °C per min, ramped to 220 °C at 4 °C per min, and held for 2 min. Pentadecanoic acid (C15:0) was used as an internal standard for calculating the concentration of individual fatty acids using chromatographic areas. All experiments were performed in three biological replicates. The statistical data were presented as mean ± S.D. Pairwise comparison of biomass and metabolites across two strains using the Student's t-test by SPSS Statistics version 22. The statistical data under p-value < 0.05 was considered a significant difference.

2.3. Measurement of Glucose and Nitrogen in the Culture Broth

The glucose concentration in the fermentation broth was determined by the glucose oxidase activity kit in accordance with the operating method provided by the manufacturer (Shanghai RongSheng Biotechnology CO., LTD., Shanghai, China). The concentration of ammonia in fermentation broth will be determined by method according to [36]. To calculate the rates of operation, glucose consumption (Q_S, g/L h), and nitrogen consumption (Q_N, g/L h), each parameter was systematically analyzed using experimental data, including biomass concentration (C_X, g/L), glucose concentration (C_S, g/L), ammonium concentration (C_N, g/L), and time intervals according to Formula (2) and Formula (3), respectively.

$$Q_S = -\frac{C_{S,2} - C_{S,1}}{t_2 - t_1} \tag{2}$$

$$Q_N = -\frac{C_{N,2} - C_{N,1}}{t_2 - t_1} \tag{3}$$

The specific rates of glucose consumption (q_S, g/g h) and ammonium consumption (q_N, g/g h) were then calculated by dividing the volumetric rates with the average biomass concentration, following Formula (4) and Formula (5), respectively.

$$q_S = \frac{1}{\left(\frac{C_{X,1}+C_{X,2}}{2}\right)} Q_S \tag{4}$$

$$q_N = \frac{1}{\left(\frac{C_{X,1}+C_{X,2}}{2}\right)} Q_N \tag{5}$$

2.4. RNA Extraction, Library Preparation, Transcriptome Sequencing and Analysis

To perform transcriptome sequencing, the mycelial cells of *M. circinelloides* WJ11 and CBS277.49 strains grown at active growth in the mid-logarithmic phase (11 hr cultivation time) were harvested, immediately frozen in liquid nitrogen, and then stored at −80 °C before RNA extraction. Total RNAs were extracted using Rneasy Plant Mini Kit (Qiagen), and the quality and concentration of total RNAs were determined using Agilent 2100 bioanalyzer. Further, the cDNA library construction and transcriptome sequencing of three biological replicates for each strain were carried out using the MGISEQ-2000RS platform. The sequencing data are available in the NCBI Sequence Read Archive (SRA). The WJ11 transcriptome data can be accessed under Bioproject PRJNA1211013727 (biosamples SAMN37309028 to SAMN37309030) and the CBS277.49 data are under BioProject PRJNA1066059 (biosamples SAMN39480229 to SAMN39480231).

2.5. Read Mapping and DEGs Analysis for Functional Annotation

For read mapping, the reads of RNA-Seq data of WJ11 and CBS277.49 in this study were mapped to the *M. circinelloides* WJ11 (NCBI's Bioproject: PRJNA290220) and CBS277.49 v. 3 (JGI database: genome.jgi.doe.gov/portal/Mucci3), respectively, and afterward quantified with Salmon [37]. First, the reads were checked using FASTQC [38] and TrimGalore, which removed adapters and low-quality bases. Clean reads were then mapped to their respective references. HISAT2 v2.2.1 was used to estimate the number of mapped reads for each gene. Genes with mapped reads were analyzed to calculate FPKM (fragment per kilobase of transcript per million mapped reads). Genes with an FPKM value ≥ 1 were considered expressed genes. Differentially expressed genes (DEGs) between the two strains were identified using the DESeq2 using the R package [39,40]. Genes with a $|\log2$ (fold change)$| \geq 1$ and q-value < 0.05 were considered significant genes. The annotated

functions of these significant genes were retrieved from the KEGG (Kyoto Encyclopedia of Genes and Genomes), GO (Gene Ontology), and eggNOG databases.

2.6. Reporter Metabolic Routes Based on the Integration Analysis of Omics Data and Genome-Scale Metabolic Model-Driven Analysis of M. circinelloides

The genome-scale metabolic model (GSMM) of *M. circinelloides* WJ11 (*i*NI1159) [27] was downloaded and used to identify reporter metabolites and highly correlated metabolic subnetworks for pairwise strain comparisons using the reporter metabolites algorithm and subnetwork analysis under the PIANO R package [41,42]. The reporter metabolites algorithm is a robust computational method for identifying key metabolites linked to global metabolic responses in a metabolic network. By utilizing high-throughput omics data, such as transcriptomics throughout this study, the algorithm highlights reporter metabolites around which the most significant transcriptional changes occur, and a set of connected genes with significant and coordinated responses to genetic or environmental perturbations, offering insights into global metabolic shifts [41]. To elaborate, the GSMM as a scaffold was integrated with the DEGs data, differentially expressed proteins (DEPs) data [31], or ^{13}C-metabolic flux data [23] for both WJ11 and CBS277.49 strains. A list of significantly upregulated metabolites, identified by directional p-values < 0.05, was considered as reporter metabolites. Additionally, a set of reporter genes and reporter enzymes, along with their corresponding reporter reactions associated with key metabolites, was identified as a potential metabolic route.

3. Results and Discussion

3.1. Comparative Growth Profiles and Targeted Metabolite Traits of M. circinelloides WJ11 and CBS277.49 Strains

The comparative growth characteristics and the lipid production of *M. circinelloides* WJ11 (high lipid-producing strain) and CBS277.49 (low lipid-producing strain) are shown in Table 1, Figure S1, and Supplementary File S1. As shown in Table 1 and Supplementary File S1, the WJ11 culture had a maximum specific growth rate (0.340 ± 0.104 h^{-1}) higher than the CBS277.49 culture (0.236 ± 0.124 h^{-1}), consistent with findings from the previous studies [21,43]. Although rapid growth (active growth phase) was found during the first 24 h of WJ11 cultivation, the biomass titers afterward were not much different. The highest biomass of WJ11 and CBS277.49 were 12.95 ± 0.6 and 12.07 ± 1.07 g/L, respectively (Table 1 and Supplementary File S1). After 24 h of cultivation, the glucose consumption rates of the CBS277.49 culture were higher than those of the WJ11 culture (Supplementary File S1). Obviously, the glucose consumption rates of both strains after 72 h of cultivation are significantly different. The glucose consumption rate of the CBS277.49 culture decreased faster than the WJ11 culture after 30 h of cultivation. Earlier studies have pointed out that when the carbon source is sufficient and the nitrogen element is insufficient, the microorganisms no longer carry out cell reproduction but convert the excess carbon source into fatty acids for storage in the form of a lipid body in the cells [44].

Table 1. Comparative growth characteristics and lipid production between *M. circinelloides* WJ11 and CBS277.49.

Parameters	WJ11	CBS277.49
Maximum specific growth rate, μmax (h^{-1})	0.340 ± 0.104	0.236 ± 0.124
Maximal biomass titer (g/L)	12.95 ± 0.6	12.07 ± 1.07
Maximal lipid (% total fatty acids (TFAs)/DCW)	35.18	13.19

Note: Maximum specific growth rate was calculated at 3–7 h.

Thus, we cultivated the fungi under excess carbon conditions to obtain high lipid-accumulating cultures. It was found that the CBS277.49 strain exhibited a low nitrogen consumption rate, with nitrogen depletion found in the 24 h culture, whereas the WJ11 strain completely consumed nitrogen after 12 h of cultivation. It can be seen that the ammonia concentration of the WJ11 cultures decreased significantly faster than that of the CBS277.49 cultures, whereas the high lipid-producing strain (WJ11) consumed glucose slower than the CBS277.49 strain after 24 h of cultivation (Supplementary File S1), indicating its efficient glucose consumption for either biomass or energy production. As seen in Figure 1 and Supplementary File S2, the lipid content (shown as TFA) of the WJ11 strain was 35.18% in DCW, which was higher than the CBS277.49 strain (13.19% TFA in DCW), similar to the previous report [20]. The lipid contents of the 48, 72, and 96 h cultures of WJ11 were significantly different, consistent with earlier reports, mentioning that the high lipid-producing strain entered the lipid accumulating phase after nitrogen depletion [21] (Supplementary File S2).

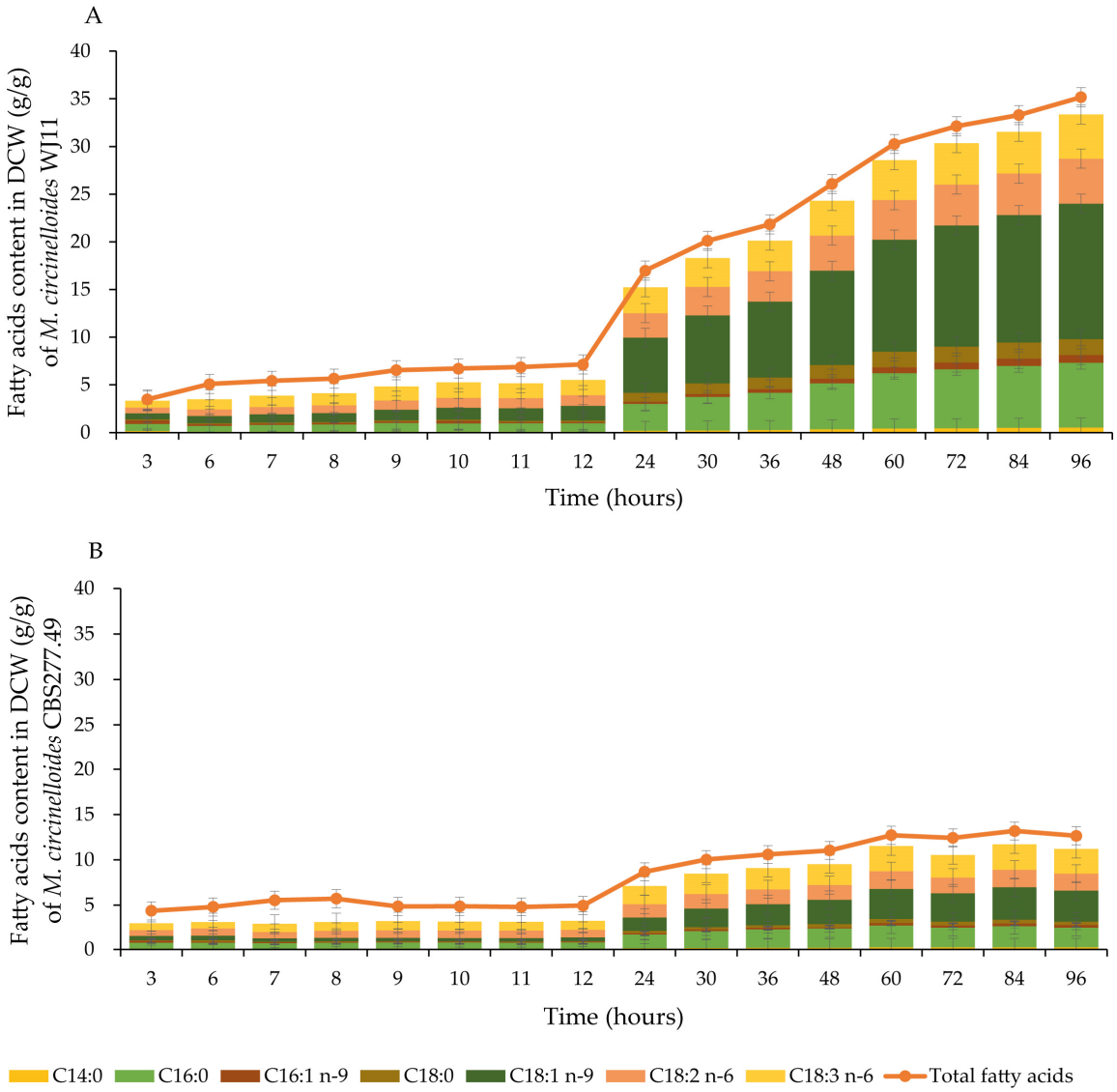

Figure 1. Comparative profiles of the fatty acid composition of *M. circinelloides* strains, (**A**) WJ11, and (**B**) CBS277.49. The values are means with standard deviations.

As shown in Figure 1 and Supplementary File S2, the TFA content of the WJ11 culture was higher than that of the CBS277.49 culture, particularly after 24 h of cultivation, where

the nitrogen was depleted. The fatty acid profiles of WJ11 and CBS277.49 were significantly different. At the lipid accumulating phase (after 24 h cultivation), the oleic acid (C18:1 *n*-9) of the WJ11 culture was higher than that of CBS277.49. Similarly, the C18:3 *n*-6 (GLA) of the WJ11 culture (4.63% in DCW) was also higher than that of the CBS277.49 culture (Figure 1). It has been reported that when fungal cells enter a state of nitrogen depletion, citric acid produced by the tricarboxylic acid cycle (TCA cycle) is no longer fully oxidized within the cycle but begins to accumulate in the cells. Then, ATP citrate lyase catalyzes the conversion of citrate and Coenzyme A (CoA) to oxaloacetate and acetyl-CoA, a key precursor for newly synthesizing fatty acids [9]. It has been previously reported that citric acid accumulation in microorganisms might be governed by nitrogen source depletion, e.g., in *Yarrowia lipolytica* strains [45] and methanol in synthetic media containing galactose. In addition, methyl alcohol enhanced production via the inhibition of 2-oxoglutarate dehydrogenase in *Aspergillus niger* [46,47] as well as oxygen levels and temperature [48,49] throughout wild-type and engineered strains [50]. The lipid physiology and the defined culture stages of the two fungal strains were then used for further study of cellular metabolisms of these fungi by comparative transcriptome analysis.

3.2. Comparative Transcriptome and Functional Analysis of WJ11 and CBS277.49 Cultures

The regulatory mechanism of the lipid-accumulating process has been extensively studied [9,17]. However, there are no reports on how oleaginous fungi optimize biomass and lipid production at a systems level. Thus, this study focused on the growth performance of the WJ11 strain at the rapid growth stage in relation to lipid metabolism. The mycelial samples harvested at the mid-logarithmic phase (11 h of cultivation) were studied to investigate the global transcriptional responses of two strains in comparison. The transcriptome analysis of WJ11 and CBS277.49 strains showed that raw reads were obtained at an average sequencing depth of 43.18 and 42.65 million reads for WJ11 and CBS277.49 strains, respectively. After removing the adaptor, low-quality sequences, and read pollution, clean reads were retrieved with an average sequencing depth of 42.95 and 42.54 million reads for WJ11 and CBS277.49 strains, respectively. The total mapped reads were 96.53% and 97.72% for WJ11 and CBS277.49 strains, respectively. The expressed genes for the WJ11 and CBS277.49 cultures were 6389 and 6008, respectively (Table 2 and Supplementary File S3). Among the total number of expressed genes, 6708 orthologous protein-encoding genes were gained according to the GO and KEGG databases (Supplementary File S4) [51–54]. Of these genes, the protein functions could be predicted for 4277 based on GO and 4257 based on KEGG Orthology (KO) (Supplementary File S5).

Table 2. Sequencing results of *M. circinelloides* WJ11 and CBS277.49 transcriptomes.

Features	WJ11	CBS277.49
Sequencing depth of raw reads (million reads)	43.18	42.65
Sequencing depth of clean reads (million reads)	42.95	42.54
Total mapped reads	96.53	97.72
Number of expressed genes	6389	6008
Total number of orthologous protein-encoding genes	6708	

Based on comparative transcriptome analysis, if FPKM value ≥ 1, they were considered expressed genes. Interestingly, the high common expression was 5944 genes, accounting for 92.1% between high lipid-producing WJ11 and low lipid-producing CBS277.49 strains (Figure 2A). It has been reported that the degree of gene identity and gene order of the two strains have common characteristics, as indicated by genomic analysis [20,55]. Our results showed that the WJ11 culture had 445 genes (6.9%) with unique expression,

whereas the CBS277.49 culture had only 64 genes (1%) with unique expression (Figure 2A). Probably, the strain-specific metabolic adaptations or regulatory variations related to their capacity for lipid generation were elaborated by differential transcriptional responses. The WJ11 strain contained a higher number of genes encoding hexokinase in the glycolysis pathway and glucose-6-phosphate dehydrogenase (G6PDH) in the pentose phosphate pathway (PPP) than the CBS 277.49 strain, which possibly directed NADPH supply to fatty acid synthesis [55].

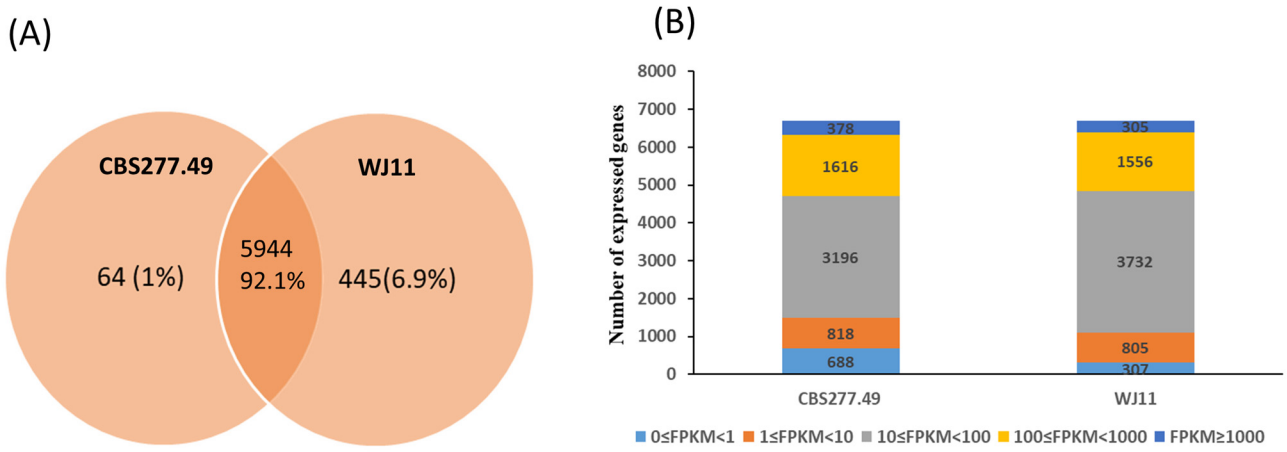

Figure 2. Comparative gene expression of transcriptomes of *M. circinelloides* CBS277.49 and *M. circinelloides* WJ11 cultures. (**A**) Venn diagram showing the expressed genes unique and common to each strain of *M. circinelloides.* (**B**) Quantification of gene expression levels in each strain based on different FPKM thresholds.

To compare the gene expression levels (GELs) between the WJ11 and CBS277.49 cultures, the expressed genes were categorized into five groups based on FPKM values: very high expression level (VHEL, FPKM $\geq$ 1000), high expression level (HEL, 100 $\leq$ FPKM < 1000), medium expression level (MEL, 10 $\leq$ FPKM < 100), low expression level (LEL, 1 $\leq$ FPKM < 10), and very low expression level (VLEL, 0 $\leq$ FPKM < 1) (Figure 2B and Supplementary File S6). Both strains had distinctive GEL profiles, and most of the genes fall into MEL, followed by HEL, LEL, and VHEL groups. This indicates that GELs were differentially regulated in each strain, referring to strain-specific regulatory mechanisms that might contribute to discrimination in lipid production between the two strains. It is noted that the CBS277.49 culture had less active transcriptome, as evidenced by the high number of genes related to the VLEL group, i.e., 688 genes.

The result of functional annotation across several protein databases upon KEGG classification is provided. Accordingly, the functions of expressed genes were classified into five major categories as seen in Figure 3A and Supplementary File S7, including metabolism (1252 genes in WJ11 and 1187 genes in CBS277.49), genetic information processing (874 genes in WJ11 and 863 genes in CBS277.49), environmental information processing (286 genes in WJ11 and 269 genes in CBS277.49), cellular processes (287 genes in WJ11 and 275 genes in CBS277.49), and organismal systems (98 genes in WJ11 and 92 genes in CBS277.49). Within the top list of metabolic sub-categories (Figure 3B and Supplementary File S8), the WJ11 culture consistently expressed the genes involved in lipid metabolism (182 genes), amino acid metabolism (155 genes), and carbohydrate metabolism (411 genes) with a higher number over another strain. These findings are in line with the enhanced capacity for lipid production of the WJ11 strain, as lipid biosynthesis involves lipid, amino acid, and carbohydrate metabolisms [20].

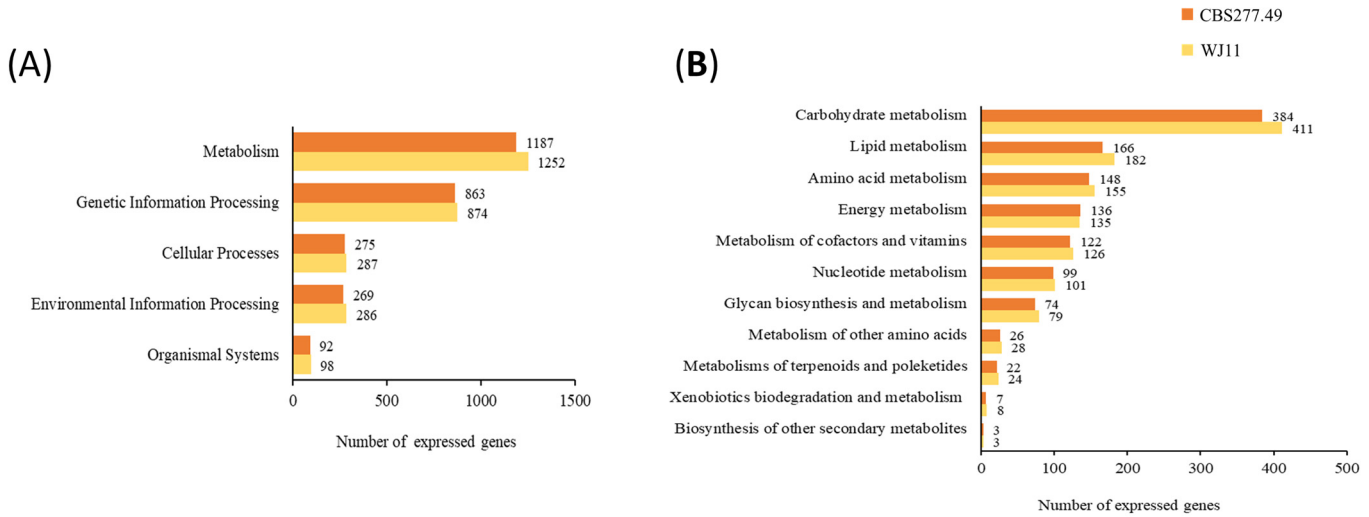

Figure 3. Distribution of functional expressed genes in *M. circinelloides* W11 and CBS277.49. (**A**) Different major functional categories of KEGG-expressed genes (**B**) Different sub-metabolic functional categories.

Carbohydrates, lipids, and amino acids are vital metabolic compounds serving as the foundation for microbial growth and development [56]. In carbohydrate metabolism, glycolysis is capable of generating ATP, which is an energy source for living cells [57,58]. The PPP in fungal cells also supply intermediates for nucleotide biosynthesis [59]. Another crucial pathway of carbohydrate metabolism is the TCA cycle [60].

As noted, the expression of gene numbers in WJ11 was similar to that in CBS277.49, including those involved in energy metabolism, metabolism of cofactors and vitamins, nucleotide metabolism, glycan biosynthesis, and metabolism, metabolism of other amino acids, metabolism of terpenoids and polyketides, xenobiotics biodegradation and metabolism, and the biosynthesis of different secondary metabolites. These may reflect the robust phenotype of these *Mucor* strains with adaptability to environmental stimuli for regulating cellular activities and lipid biosynthesis [22].

3.3. Identification of Significant Genes Involved in Lipid Metabolic Responses Using DEGs Analysis of WJ11 and CBS277.49 Strains

The total number of orthologous protein-encoding genes (6708 genes) was compared to the expressed genes of WJ11 (6389 genes) and CBS277.49 (6008 genes) (Table 2). A comparative DEG analysis was then conducted for the two strains, WJ11 and CBS277.49. As a result, 2811 significant genes with 1569 upregulated and 1242 downregulated genes were identified under thresholds $|\log2FC| \geq 1$ and q-value < 0.05, as illustrated in Figure 4A and Supplementary File S9. An expression volcano plot of both upregulated and downregulated DEGs is illustrated in Figure 4B. The significant genes were classified based on KEGG to explore the critical attributes in the transcriptional regulation of WJ11 and CBS277.49 strains (Figure 4C and Supplementary File S10). Interestingly, the top three lists of significantly upregulated genes were found in carbohydrate metabolism (133 genes), lipid metabolism (61 genes), and amino acid metabolism (31 genes).

Of these top three functional categories (Figure 4C), the key significant upregulated genes involved in lipid metabolic responses were searched across sub-metabolic functional categories with solid fold change ($|\log2FC| \geq 5$). As a result, we found 63 key orthologous genes involved in metabolic responses, of which 18 genes were linked to energy production, lipid metabolism, and cellular function, e.g., precursor and NADPH/ATP supply, as shown in Table 3 and Supplementary File S11.

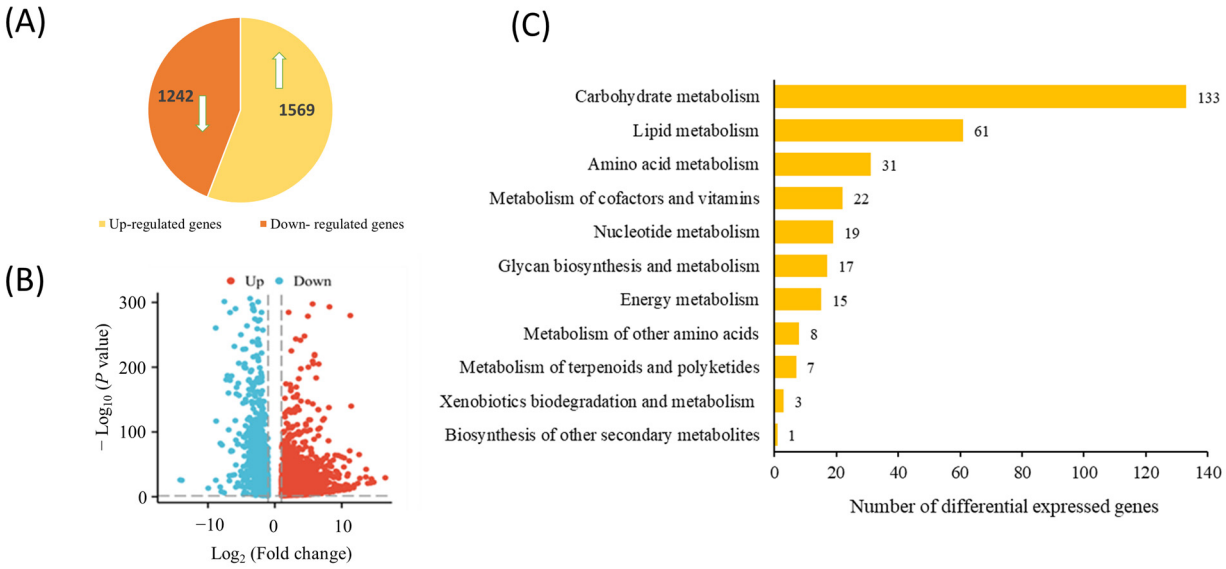

Figure 4. Comparative DEGs analysis between *M. circinelloides* WJ11 and CBS277.49 strains. (**A**) Pie chart showing the distribution of upregulated and downregulated genes in the WJ11 culture compared to the CBS277.49 culture. (**B**) Volcano plot of differentially expressed genes identified between the two strains. (**C**) Significant genes associated with the top list of metabolic categories.

Table 3. A comparison of key significant genes and their enzymes involved in central carbon metabolism towards amino acid and lipid metabolism identified in *M. circinelloides* strain WJ11 compared with the strain CBS277.49.

Orthologous Gene ID	Log_2FC	Protein Function	EC Number
List of upregulated genes in WJ11			
1. Carbohydrate metabolism			
1.1 Glycolysis/Gluconeogenesis			
ortholog_01035	5.41	Belongs to the hexokinase family	EC: 2.7.1.1
ortholog_01766	5.54	Belongs to the aldehyde dehydrogenase family (ALDH)	EC: 1.2.1.3, EC: 1.2.1.5, EC: 1.2.1.28
ortholog_03743	8.79	Zinc-binding alcohol dehydrogenase	EC: 1.1.1.2
ortholog_04422	6.00	Aldo/keto reductase family	EC: 1.1.1.21
ortholog_05383	9.62	Phosphoenolpyruvate carboxykinase (ATP)	EC: 4.1.1.49
ortholog_05948	11.42	Aldehyde dehydrogenase family (ALDH)	EC: 1.2.1.3, EC: 1.2.1.314
ortholog_06385	5.83	Pyruvate decarboxylase	EC: 4.1.1.1
1.2 Citrate cycle (TCA cycle)			
ortholog_00844	6.52	2-oxoglutarate dehydrogenase E2 component (dihydrolipoamide succinyltransferase)	EC: 2.3.1.61
2. Lipid metabolism			

Table 3. *Cont.*

Orthologous Gene ID	Log_2FC	Protein Function	EC Number
2.1 Fatty acid biosynthesis/degradation			
ortholog_03018	6.41	Acyl-CoA synthetase	EC: 6.2.1.3
ortholog_05253	6.42	AMP-binding enzyme (Acyl-CoA synthetase)	EC: 6.2.1.3
ortholog_03225	7.44	Hypothetical protein	-
2.2 Glycerophospholipid metabolism			
ortholog_01371	7.49	GDSL-like Lipase/Acylhydrolase	EC: 3.1.1.4, EC: 3.1.1.5
ortholog_04515	11.09	Protein of unknown function (DUF3419)	-
3. Amino acid metabolism			
3.1 Phenylalanine metabolism			
ortholog_01802	5.65	Biopterin-dependent aromatic amino acid hydroxylase	EC: 1.14.16.1, EC: 1.14.16.2, EC: 1.14.16.4
3.2 Tryptophan metabolism			
ortholog_03575	6.13	Indoleamine 2,3-dioxygenase	EC: 1.13.11.52
3.3 Lysine degradation			
ortholog_04503	8.17	Dehydrogenase E1 and transketolase domain-containing protein 1	EC: 1.2.4.2
4. Secondary metabolism			
ortholog_00981	6.19	Squalene/phytoene synthase	EC: 2.5.1.21, 2.5.1.32
ortholog_01138	8.44	Carotenoid-9′,10′-cleaving dioxygenase	EC: 1.13.11.71
List of upregulated genes in CBS277.49			
1. Carbohydrate metabolism			
1.1 Glycolysis/Gluconeogenesis			
ortholog_03434	5.48	Glyceraldehyde 3-phosphate dehydrogenase, NAD binding domain	EC: 1.2.1.12
1.2 Pyruvate metabolism			
ortholog_03454	8.83	HMGL-like (Isopropylmalate synthase, homocitrate synthase)	EC: 2.3.3.13, EC: 2.3.3.14
1.3 Citrate cycle (TCA cycle)			
ortholog_04943	6.68	Isocitrate/isopropyl malate dehydrogenase	EC: 1.1.1.41, EC: 1.1.1.87
2. Lipid metabolism			
2.1 Arachidonic acid metabolism			
ortholog_00884	5.74	Asparagine synthase	EC: 3.3.2.6, EC: 6.3.5.4
2.2 Glycerolipid metabolism			
ortholog_02135	13.91	Triacylglycerol lipase	EC: 3.1.1.3
3. Amino acid metabolism			

Table 3. *Cont.*

Orthologous Gene ID	Log_2FC	Protein Function	EC Number
3.1 Lysine biosynthesis			
ortholog_05309	5.71	Homoaconitate hydratase	EC: 4.2.1.36
3.2 Alanine, aspartate, and glutamate metabolism			
ortholog_06359	5.38	Arginosuccinate synthase	EC: 6.3.4.5

Note: The selected list of significant genes is considered under $|log2FC| \geq 5$ and q-value < 0.05 under manual curation. Full information is available in Supplementary File S11. The orthologous Gene ID is shown in Supplementary File S4.

In glycolysis/gluconeogenesis (7 genes) and TCA cycle (1 gene), notably ortholog_01035, a hexokinase family member (EC: 2.7.1.1), plays a role in glucose metabolism for producing ATP. Ortholog_01766 and ortholog_05948 from the aldehyde dehydrogenase family (EC: 1.2.1.5, 1.2.1.3, 1.2.2.28, 1.2.1.31), ortholog_03743, which encoded zinc-binding alcohol dehydrogenase (EC: 1.1.1.2), and ortholog_04422, which encoded aldo/keto reductase (EC: 1.1.1.21), were involved in redox reactions involved in the generation of reducing equivalents for NADH and NADPH [61] supply and biosynthesis pathway [62].

Additionally, ortholog_05383, a phosphoenolpyruvate carboxykinase, generates ATP (EC: 4.1.1.49), which is crucial for gluconeogenesis and glycerol production supporting cellular energy requirement. Ortholog_06385 encoded pyruvate decarboxylase (EC: 4.1.1.1), which converts pyruvate to acetaldehyde, providing precursors for fatty acid synthesis. Additionally, ortholog_00844 encoded 2-oxoglutarate dehydrogenase (EC: 2.3.1.61), essential in the TCA cycle, and ortholog_01138 encoded carotenoid cleavage dioxygenase (EC: 1.13.11.71), which cleaves carotenoids into colorless compounds. These enzymes collectively contribute to cellular energy balance and metabolic homeostasis.

Several genes were highlighted in fatty acid biosynthesis, degradation, and glycerophospholipid metabolism. In the fatty acid metabolism, ortholog_03018 encoded acyl-CoA synthetase (EC: 6.2.1.3), which is essential for the activation of fatty acids, de novo complex lipid biosynthesis, fatty acid β-oxidation, post-translational modification of proteins, and membrane biogenesis [63], while ortholog_05253, an AMP-binding enzyme, likely plays a role in energy regulation during these metabolic processes. Ortholog_03225 also contributes to fatty acid metabolism, further supporting the cellular capacity for fatty acid synthesis or degradation. In glycerophospholipid metabolism, ortholog_01371 encoded a GDSL-like lipase/acylhydrolase (EC: 3.1.1.4, EC: 3.1.1.5), which is involved in the hydrolysis of lipids, likely impacting membrane structure and function. These orthologs collectively contribute to essential lipid-related pathways, influencing cellular energy balance, membrane integrity, and overall metabolic regulation.

Further functional analysis of amino acid metabolism also revealed an intricate link to lipid metabolic responses. The enzymes involved in phenylalanine, tryptophan, and lysine metabolism are critical for amino acid catabolism and regulate lipid homeostasis. In phenylalanine metabolism, ortholog_01802, a biopterin-dependent aromatic amino acid hydroxylase (EC: 1.14.16.1, 1.14.16.2, 1.14.16.4), contributes to the synthesis of key metabolites that influence lipid signaling pathways. In tryptophan metabolism, ortholog_03575, encoding indoleamine 2,3-dioxygenase (EC: 1.13.11.52), has been shown to regulate the balance of bioactive molecules that may impact lipid metabolism, mainly through the kynurenine pathway. Additionally, ortholog_04503, a dehydrogenase E1 and transketolase domain-containing protein 1 (EC: 1.2.4.2), connects lysine catabolism with central metabolic pathways, influencing the synthesis and degradation of lipids, as well as cellular energy maintenance. Additionally, ortholog_00981 encoded squalene/phytoene synthase (EC: 2.5.1.21, 2.5.1.32), which plays a significant role in secondary metabolism by generating

sterols, carotenoids, and other terpenoid compounds. This enzyme is essential for the biosynthesis of squalene and phytoene in which phytoene synthase (PSY) catalyzes the first step of the carotenoid biosynthesis pathway and is also a key rate-limiting enzyme of carotenogenesis [64].

Altogether, these metabolic pathways were interconnected, and the enzymes involved in the coordinated regulation of both amino acid and lipid metabolisms, ensuring cellular energy homeostasis and efficient metabolic function to lipid overproduction. Of 15 upregulated genes encoding key enzymes in metabolic responses, only 7 genes were identified in carbohydrate, amino acid, and lipid metabolisms of the CBS277.49 strain (Supplementary File S11). In carbohydrate metabolism, it supports enhanced NADH supply for cell growth. In pyruvate mechanism, ortholog_03454, encoding either isopropyl malate synthase (IPMS; EC: 2.3.3.13) or homocitrate synthase (HCS; EC: 2.3.3.14), catalyzes acetyl-CoA and 2-oxoglutarate to form isopropyl malate (first step of leucine biosynthesis) or homocitrate (first step of lysine biosynthesis), thereby facilitating fatty acids and oligopeptides production [65,66]. In glycolysis, ortholog_03434, encoding glyceraldehyde 3-phosphate dehydrogenase (EC: 1.2.1.12), catalyzes the NAD^+-dependent conversion of glyceraldehyde 3-phosphate to 1,3-bisphosphoglycerate, generating NADH [67]. This suggests an increased glycolytic flux for enhancing NADH production in cellular processes. Additionally, in the citrate cycle, ortholog_04943, encoding isocitrate dehydrogenase (EC: 1.1.1.41), responsible for the NADH generation through the oxidation of isocitrate, further supporting the NADH supply required for ATP synthesis and cellular growth. Concerning glycerolipid metabolism, notably ortholog_02135 encoding triacylglycerol lipase (TGL) (EC: 3.1.1.3) in CBS277.49 was significantly upregulated. TGL hydrolyzes triacylglycerol to diacylglycerol, monoacylglycerol, and free fatty acids [68], supporting the energy balance in cells [69].

Amino acids play a crucial role in supporting cell growth and protein synthesis [70]. In the CBS277.49 strain, asparagine synthase (EC: 6.3.5.4) was significantly upregulated, enhancing the conversion of nitrogen and aspartate into asparagine, an essential amino acid required for protein production and cell proliferation. Furthermore, ortholog_06359, encoding arginosuccinate synthase (ASS) (EC: 6.3.4.5), which catalyzes a key step in the urea cycle and arginine biosynthesis was significantly upregulated, highlighting its important role in cell growth and repair as reported for *Aspergillus nidulans* [71].

In addition, ortholog_05309, encoding homoaconitate hydratase (EC: 4.2.1.36), was upregulated in lysine biosynthesis, facilitating the synthesis of lysine through the alpha-aminoadipic acid pathway [72], further supporting cellular function and growth. As critical building blocks, these amino acids contribute to synthesizing proteins that are fundamental for cell division, metabolism, and overall cellular growth.

3.4. Identified Reporter Metabolic Routes in M. circinelloides Strain WJ11 for the Fast-Growing Stage with Its Lipid Production Using Integrated Omics Data and Genome-Scale Model-Driven Analysis

To analyze the global metabolic responses on strain dependence, i.e., WJ11 versus CBS277.49, we applied the reporter algorithm to identify reporter metabolites and enzymes and search for highly correlated metabolic subnetworks. The pairwise strain comparisons relied on the genome-scale metabolic model of *M. circinelloides* WJ11 (*i*NI1159 model) [27], demonstrating how the metabolic network can map the global regulatory response of *M. circinelloides*. The top 20 significant reporter metabolites affected by transcriptional up-regulation in WJ11 response compared to CBS277.49 culture are listed in Table 4 and Supplementary File S12. Considering lipid production, these metabolites made sense biologically since the identified reporter metabolites were related to all possible main precursors and intermediate metabolites involved in carbohydrate metabolism,

amino acid metabolism, energy metabolism, and one-carbon metabolism towards lipid metabolism, including 2-oxoglutarate (AKG), diphosphate (PPI), phosphate (PI), H(+), ATP, ubiquinol (QH2), ubiquinone (Q), AMP, L-aspartate (ASP), L-glutamate (GLU), transfer RNA (TRNA), NAD(+), FAD, $FADH_2$, tetrahydrofolate (THF), S-adenosyl-L-methionine (SAM), L-homocysteine (HCYS), L-glutamine (GLN), S-adenosyl-L-homocysteine (SAH), NADH, and O-acetyl-L-homoserine (OAHSER).

Table 4. List of top 20 reporter metabolites with up-directional changes in WJ11 culture at the active growth phase.

Reporter Metabolites	Distinct-Directional *p*-Value
2-oxoglutarate	0.014925 *
diphosphate	0.014925 *
Phosphate	0.014925 *
H^+	0.014925 *
ATP	0.014925 *
Ubiquinol	0.014925 *
Ubiquinone	0.014925 *
AMP	0.014925 *
L-aspartate	0.014925 *
L-glutamate	0.014925 *
transfer RNA	0.014925 *
NAD^+	0.014925 *
FAD^+	0.014925 *
tetrahydrofolate	0.014925 *
S-adenosyl-L-methionine	0.014925 *
L-homocysteine	0.014925 *
L-glutamine	0.026118 *
S-adenosyl-L-homocysteine	0.026118 *
NADH	0.033581 *
O-acetyl-L-homoserine	0.033581 *

Note: The metabolite with a distinct up-directional *p*-value < 0.05 was identified as a significant reporter metabolite (*).

The key metabolic routes were curated by integrated data analysis. Interestingly, the central carbon metabolism, i.e., glycolysis, the TCA cycle, and amino acid metabolism (e.g., leucine degradation and alanine metabolism), in connection with fatty acids and lipid biosynthetic routes identified in WJ11, as illustrated in Figure 5. Using the identified expressed genes and involved metabolites to compare the biochemical activities between the two strains, we found lower carbon fluxes in WJ11 to the TCA cycle rather than in acetyl-CoA for lipid biosynthesis, corresponding to its higher lipid production compared to the CBS 277.49 strain. The list of upregulated genes encoding glycolytic enzymes in WJ11 included aldehyde dehydrogenase, hexokinase, glyceraldehyde-3-phosphate dehydrogenase, pyruvate kinase, and the aldo/keto reductase family.

The genes involved in methionine metabolism were significantly downregulated (Figure 5, Supplementary File S13). It has been reported that downregulation of the methionine cycle and tricarboxylic acid cycle led to more carbon flow toward fatty acid biosynthesis, glycerolipid, and glycerophospholipid metabolism, and also to rapid synthesis of other amino acids, such as arginine, alanine, and aspartate. When methionine was restricted, acetyl-CoA stimulated the metabolism of α-ketoglutarate-glutamate-arginine by activating glutamate [73].

One-carbon metabolism includes the folate cycle, methionine cycle, and transsulfuration pathway, which is a complex cyclic metabolic network based on folic acid compounds [74,75]. A carbon metabolic pathway can function with folate and methionine cycles, contributing to nucleotide synthesis, lipid metabolism, and cellular redox

balance [76]. One-carbon metabolism supports the synthesis of porphyrin, thymine, purine, glutathione (GSH), and S-adenosyl-L-methionine (SAM). SAM is a one-carbon donor for synthesizing lipids, histones, and DNA methylation metabolites. The SAM depletion in yeast cells affected the coordination mechanism of energy metabolism and anabolism [73]. When SAM was depleted, other amino acids were rapidly synthesized, resulting in a large accumulation of amino acids, especially arginine, to promote cell growth. The serine synthesis pathway (SSP pathway) produces glycine through serine hydroxymethyltransferase (SHMT) [77] to provide a carbon source for one-carbon metabolism. Moreover, serine is also an important precursor of several biomolecules for cell proliferation, such as the synthesis of cysteine, glycine, nucleotides, and folate [78]. Our results in the transcriptome analysis indicated the synergistic function of these metabolic processes for fungal membrane structure and cell proliferation [79,80]. Fungal cell walls consist of various glucans and chitin, and chitinase is required to enlarge the cell wall surface area during hyphal growth. In the WJ11 strain, the expressed genes (e.g., chitin synthase, chitinase, and chitin deacetylase) were predominant in the active growth phase and might be involved in chitin metabolism during its growth. Interestingly, the expressed genes encoding phosphatidylserine decarboxylase and protein-serine/threonine phosphatase were detected in WJ11. These enzymes are essential for cell wall integrity, virulence, and cell growth.

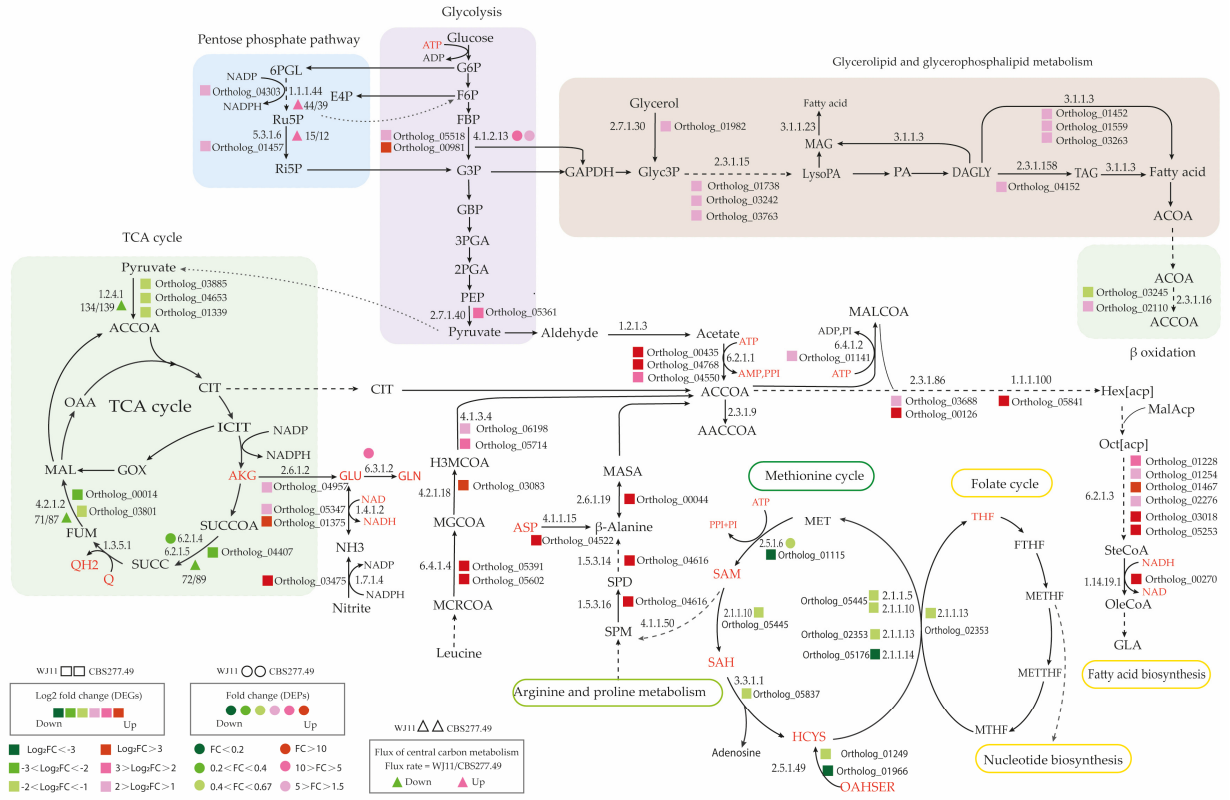

Figure 5. Proposed potential metabolic routes identified in high lipid-producing *M. circinelloides* WJ11. Note: The selected highlight genes are considered in this proposed route. Full information and abbreviations are provided in Supplementary Files S13 and S14, respectively. The dash line arrow shows multiple steps. The dot line arrow shows a transport. The solid line arrow shows a single metabolic reaction. The red letter is reporter metabolite.

For energy supply, the glucose-6-phosphate dehydrogenase (G6PDH) gene was up-regulated in the WJ11 strain. It has been documented that NADPH generated from the pentose phosphate pathway plays a key role in lipid accumulation in *Yarrowia lipolytica*, *Mortierella alpina*, and *Fistulifera solaris* [31,81–83]. The result in Table 4 also supports the role

of high-energy compounds (NAD+, FAD+, NADH, and ATP) in cellular energy metabolism, particularly in supporting the cell growth, biosynthesis and degradation, and metabolic flexibility of the WJ11 strain.

This research provides valuable insights into the regulatory mechanisms of lipid production and potential metabolic pathways to optimize the high lipid-producing *M. circinelloides* strain WJ11. Though it may be outperformed by other genera/species, e.g., thraustochytrids [84], microalgae [85], and *Yarrowia lipolytica* [45], these findings could help improve lipid production and expand microbial options for industrial use [45,84,85]. Further metabolomics, metabolic engineering, and strain optimization of *M. circinelloides* WJ11 are required for establishing efficient fungal cell factories in lipid biotechnology.

4. Conclusions

Our study highlighted strain-dependent differences in growth behavior and lipid production of *M. circinelloides* at the fast-growing stage, driven by transcriptional regulation across key metabolic pathways. Through genome-scale model-driven analysis, we identified 20 significant reporter metabolites that provide insights into the mechanisms employed by the WJ11 strain to optimize growth for lipid overproduction in the subsequent lipid-accumulating stage. These mechanisms primarily involve energy, carbohydrates, amino acids, and one-carbon metabolisms. These findings open new possibilities for the precise manipulation of *M. circinelloides* WJ11, paving the way for the efficient production of high-value lipid-derived products with industrial applications.

Supplementary Materials: The following supporting information can be downloaded at: https://www.mdpi.com/article/10.3390/fermentation11020061/s1, Supplementary File S1. Growth characteristics and lipid production between *M. circinelloides* WJ11 and CBS277.49; Supplementary File S2. List of total fatty acid and fatty acid composition of *M. circinelloides* WJ11 and CBS277.49; Supplementary File S3. List of expressed genes of *M. circinelloides* WJ11 and CBS277.49; Supplementary File S4. List of orthologous protein-encoding genes of *M. circinelloides*; Supplementary File S5. Annotation by KEGG and GO; Supplementary File S6. Gene expression levels between the strain CBS277.49 and WJ11 of *M. circinelloides*; Supplementary File S7. List of annotated genes expressed in different categories of WJ11 strain and CBS277.49 strain of *M. circinelloides*; Supplementary File S8. List of annotated genes expressed in the metabolic category of *M. circinelloides* in WJ11 strain and CBS277.49 strain; Supplementary File S9. List of upregulated and downregulated genes; Supplementary File S10. List of annotated genes expressed in metabolic subcategory by DEGs; Supplementary File S11. High fold-change genes involved in the metabolic pathways; Supplementary File S12. List of reporter metabolites in *M. circinelloides* WJ11; Supplementary File S13. List of enzymes in Figure 5; Supplementary File S14: A list of full names of metabolites is illustrated in Figure 5. Figure S1. Growth physiological data of *M. circinelloides* strains WJ11 and CBS277.49.

Author Contributions: F.L. and N.M.P.S.H. prepared the samples, analyzed the data, prepared figures and tables, and wrote the manuscript; P.P. and J.Y. assisted in analyzing the data; K.L. co-supervised this study and discussed the results; Y.S. and W.V. conceived and designed experiments, interpreted all results, supervised throughout the study, and wrote the manuscript. All authors revised the manuscript. All authors have read and agreed to the published version of the manuscript.

Funding: This research was funded by the Natural Science Foundation of China (grant No. 31972851), and the Taishan Industrial Experts Programme (TSCY 20160101).

Data Availability Statement: Raw sequencing data are available in the National Center for Biotechnology Information Sequence Read Archive (NCBI-SRA) repository under the BioProject accession number PRJNA1013727 (BioSample: SAMN373090) and PRJNA1066059 (BioSample: SAMN394802).

Acknowledgments: The authors would like to thank the Sysbiomics team and the Office of the Ministry of Higher Education, Science, Research and Innovation, and Thailand Science Research and Innovation through the Kasetsart University Reinventing University Program 2024, as well as Kasetsart University International College. The authors would also like to thank Siwaporn Wannawilai from the National Science and Technology Development Agency (NSTDA) for assisting with experimental data analysis. F.L. would like to thank the Interdisciplinary Graduate Program in Bioscience, Faculty of Science, Kasetsart University, as well as the Colin Rateledge Center for Microbial Lipids, School of Agricultural Engineering and Food Science, Shandong University of Technology. W.V. would like to thank the Department of Zoology, SciKU Biodata Server, and International SciKU Branding (ISB), Faculty of Science, Kasetsart University, for support. PP would like to thank the Postdoctoral Fellowship Program 2024 at Kasetsart University, Kasetsart University Research and Development Institute (KURDI).

Conflicts of Interest: The authors declare no conflicts of interest.

References

1. Cao, M.; Li, X.; Zhang, B.; Han, S.; Yang, Y.; Zhou, B.; Zhang, Y. The effect of polyene phosphatidyl choline intervention on nonalcoholic steatohepatitis and related mechanism. *Am. J. Transl. Res.* **2016**, *8*, 2325–2330. [PubMed]
2. Hara, T.; Ichimura, A.; Hirasawa, A. Therapeutic role and ligands of medium- to long-chain fatty acid receptors. *Front. Endocrinol.* **2014**, *5*, 83. [CrossRef] [PubMed]
3. Yang, X.; Zhang, D.; Song, L.-M.; Xu, Q.; Li, H.; Xu, H. Chemical profile and antioxidant activity of the oil from peony seeds (*Paeonia suffruticosa* Andr.). *Oxidative Med. Cell Longev.* **2017**, *2017*, 9164905. [CrossRef] [PubMed]
4. Kothapalli, K.S.D.; Ye, K.; Gadgil, M.S.; Carlson, S.E.; O'brien, K.O.; Zhang, J.Y.; Park, H.G.; Ojukwu, K.; Zou, J.; Hyon, S.S.; et al. Positive selection on a regulatory insertion—Deletion polymorphism in *FADS2* influences apparent endogenous synthesis of arachidonic acid. *Mol. Biol. Evol.* **2016**, *33*, 1726–1739. [CrossRef] [PubMed]
5. Lund, A.S.Q.; Hasselbalch, A.L.; Gamborg, M.; Skogstrand, K.; Hougaard, D.M.; Heitmann, B.L.; Kyvik, K.O.; Sørensen, T.I.; Jess, T. N-3 polyunsaturated fatty acids, body fat and inflammation. *Obes. Facts* **2013**, *6*, 369–379. [CrossRef] [PubMed]
6. Du, H.; Huang, M.; Hu, J.; Li, J. Modification of the fatty acid composition in Arabidopsis and maize seeds using a stearoyl-acyl carrier protein desaturase-1 (ZmSAD1) gene. *BMC Plant Biol.* **2016**, *16*, 137. [CrossRef] [PubMed]
7. Sergeant, S.; Rahbar, E.; Chilton, F.H. Gamma-linolenic acid, Dihommo-gamma linolenic, eicosanoids and inflammatory processes. *Eur. J. Pharmacol.* **2016**, *785*, 77–86. [CrossRef] [PubMed]
8. Khanna, S.; Jaiswal, K.S.; Gupta, B. Managing rheumatoid arthritis with dietary interventions. *Front. Nutr.* **2017**, *4*, 52. [CrossRef] [PubMed]
9. Ratledge, C. *Microbial Production of γ-Linolenic Acid*; Functional Foods and Nutraceuticals Series; Mazza., G., Ed.; CRC Press: Boca Raton, FL, USA, 2006; p. 543.
10. Ochsenreither, K.; Glück, C.; Stressler, T.; Fischer, L.; Syldatk, C. Production strategies and applications of microbial single cell oils. *Front. Microbiol.* **2016**, *7*, 1539. [CrossRef] [PubMed]
11. Koivuranta, K.; Castillo, S.; Jouhten, P.; Ruohonen, L.; Penttilä, M.; Wiebe, M.G. Enhanced triacylglycerol production with genetically modified trichosporon oleaginosus. *Front. Microbiol.* **2018**, *9*, 1337. [CrossRef] [PubMed]
12. Kooienga, E.M.; Baugher, C.; Currin, M.; Tomberlin, J.K.; Jordan, H.R. Effects of bacterial supplementation on black soldier fly growth and development at benchtop and industrial scale. *Front. Microbiol.* **2020**, *11*, 587979. [CrossRef] [PubMed]
13. Dzurendova, S.; Zimmermann, B.; Tafintseva, V.; Kohler, A.; Ekeberg, D.; Shapaval, V. The influence of phosphorus source and the nature of nitrogen substrate on the biomass production and lipid accumulation in oleaginous Mucoromycota fungi. *Appl. Microbiol. Biotechnol.* **2020**, *104*, 8065–8076. [CrossRef]
14. Xia, C.; Zhang, J.; Zhang, W.; Hu, B. A new cultivation method for microbial oil production: Cell pelletization and lipid accumulation by *Mucor circinelloides*. *Biotechnol. Biofuels* **2011**, *4*, 15. [CrossRef] [PubMed]
15. Safe, S.; Duncan, J. Effect of oxygen levels on the fatty acids and lipids of *Mucor rouxii*. *Lipids* **1974**, *9*, 285–289. [CrossRef] [PubMed]
16. El-Gendi, H.; Saleh, A.K.; Badierah, R.; Redwan, E.M.; El-Maradny, Y.A.; El-Fakharany, E.M. A Comprehensive insight into fungal enzymes: Structure, classification, and their role in Mankind's challenges. *J. Fungi* **2021**, *8*, 23. [CrossRef] [PubMed]
17. Marchut-Mikolajczyk, O.; Kwapisz, E.; Wieczorek, D.; Antczak, T. Biodegradation of diesel oil hydrocarbons enhanced with *Mucor circinelloides* enzyme preparation. *Int. Biodeterior. Biodegradation* **2015**, *104*, 142–148. [CrossRef]
18. Majumder, R.; Miatur, S.; Saha, A.; Hossain, S. Mycoprotein: Production and nutritional aspects: A review. *Sustain. Food Technol.* **2024**, *2*, 81–91. [CrossRef]

19. Dalbanjan, N.P.; Eelager, M.P.; Narasagoudr, S.S. Microbial protein sources: A comprehensive review on the potential usage of fungi and cyanobacteria in sustainable food systems. *Food Humanit.* **2024**, *3*, 100366. [CrossRef]
20. Tang, X.; Zhao, L.; Chen, H.; Chen, Y.Q.; Chen, W.; Song, Y.; Ratledge, C. Complete genome sequence of a high lipid-producing strain of *Mucor circinelloides* wj11 and comparative genome analysis with a low lipid-producing strain CBS 277.49. *PLoS ONE* **2015**, *10*, e0137543. [CrossRef] [PubMed]
21. Tang, X.; Chen, H.; Chen, Y.Q.; Chen, W.; Garre, V.; Song, Y.; Ratledge, C. Comparison of biochemical activities between high and low lipid-producing strains of *Mucor circinelloides*: An explanation for the high oleaginicity of strain WJ11. *PLoS ONE* **2015**, *10*, e0128396. [CrossRef]
22. Tang, X.; Zan, X.; Zhao, L.; Chen, H.; Chen, Y.Q.; Chen, W.; Song, Y.; Ratledge, C. Proteomics analysis of high lipid-producing strain *Mucor circinelloides* WJ11: An explanation for the mechanism of lipid accumulation at the proteomic level. *Microb. Cell Factories* **2016**, *15*, 35. [CrossRef]
23. Zhao, L.; Zhang, H.; Wang, L.; Chen, H.; Chen, Y.Q.; Chen, W.; Song, Y. 13 C-metabolic flux analysis of lipid accumulation in the oleaginous fungus *Mucor circinelloides*. *Bioresour. Technol.* **2015**, *197*, 23–29. [CrossRef] [PubMed]
24. Vongsangnak, W.; Kingkaw, A.; Yang, J.; Song, Y.; Laoteng, K. Dissecting metabolic behavior of lipid over-producing strain of *Mucor circinelloides* through genome-scale metabolic network and multi-level data integration. *Gene* **2018**, *670*, 87–97. [CrossRef] [PubMed]
25. Thiele, I.; Palsson, B.O. A protocol for generating a high-quality genome-scale metabolic reconstruction. *Nat. Protoc.* **2010**, *5*, 93–121. [CrossRef] [PubMed]
26. Vongsangnak, W.; Klanchui, A.; Tawornsamretkit, I.; Tatiyaborwornchai, W.; Laoteng, K.; Meechai, A. Genome-scale metabolic modeling of *Mucor circinelloides* and comparative analysis with other oleaginous species. *Gene* **2016**, *583*, 121–129. [CrossRef] [PubMed]
27. Na Ayudhya, N.I.; Laoteng, K.; Song, Y.; Meechai, A.; Vongsangnak, W. Metabolic traits specific for lipid-overproducing strain of *Mucor circinelloides* WJ11 identified by genome-scale modeling approach. *PeerJ* **2019**, *7*, e7015. [CrossRef] [PubMed]
28. Naz, T.; Zhao, X.Y.; Li, S.; Saeed, T.; Ullah, S.; Nazir, Y.; Liu, Q.; Mohamed, H.; Song, Y. The interplay of transcriptional regulator SREBP1 with AMPK promotes lipid biosynthesis in *Mucor circinelloides* WJ11. *Biochim. Biophys. Acta (BBA)-Mol. Cell Biol. Lipids* **2024**, *1870*, 159592. [CrossRef]
29. Hu, H.; Li, P.; Li, S.; Wang, X.; Mohamed, H.; López-García, S.; Liu, Q.; Garre, V.; Song, Y. The role of areA in lipid accumulation in high lipid-producing fungus *Mucor circinelloides* WJ11. *Biochim. Biophys. Acta (BBA)-Mol. Cell Biol. Lipids* **2024**, *1869*, 159450. [CrossRef]
30. Wang, X.; Li, S.; Pang, S.; Liu, Q.; Song, Y. Regulation of AreA on lipid biosynthesis under different nitrogen sources and C/N ratios in the model oleaginous fungus *Mucor circinelloides*. *Biochim. Biophys. Acta (BBA)-Mol. Cell Biol. Lipids* **2024**, *1869*, 159537. [CrossRef]
31. Tang, X.; Chen, H.; Gu, Z.; Zhang, H.; Chen, Y.Q.; Song, Y.; Chen, W. Comparative Proteome analysis between high lipid-producing strain *Mucor circinelloides* WJ11 and low lipid-producing strain CBS 277.49. *J. Agric. Food Chem.* **2017**, *65*, 5074–5082. [CrossRef] [PubMed]
32. Kendrick, A.; Ratledge, C. Desaturation of polyunsaturated fatty acids in *Mucor circinelloides* and the involvement of a novel membrane-bound malic enzyme. *Eur. J. Biochem.* **1992**, *209*, 667–673. [CrossRef]
33. Yang, J.; Khan, A.K.; Zhang, H.; Zhang, Y.; Certik, M.; Garre, V.; Song, Y. Mitochondrial citrate transport system in the fungus *Mucor circinelloides*: Identification, phylogenetic analysis, and expression profiling during growth and lipid accumulation. *Curr. Microbiol.* **2020**, *77*, 220–231. [CrossRef] [PubMed]
34. Khan, A.K.; Yang, J.; Hussain, S.A.; Zhang, H.; Garre, V.; Song, Y. Genetic Modification of *Mucor circinelloides* to construct stearidonic acid producing cell factory. *Int. J. Mol. Sci.* **2019**, *20*, 1683. [CrossRef]
35. Khan, A.K.; Yang, J.; Hussain, S.A.; Zhang, H.; Liang, L.; Garre, V.; Song, Y. Construction of DGLA producing cell factory by genetic modification of *Mucor circinelloides*. *Microb. Cell Factories* **2019**, *18*, 64. [CrossRef]
36. Chaney, A.L.; Marbach, E.P. Modified reagents for determination of urea and ammonia. *Clin. Chem.* **1962**, *8*, 130–132. [CrossRef] [PubMed]
37. Patro, R.; Duggal, G.; Kingsford, C. Salmon: Accurate, versatile and ultrafast quantification from RNA-seq data using lightweight-alignment. *BioRxiv* **2015**, *10*, 021592.
38. FastQC, A. Quality Control Tool for High Throughput Sequence Data. BibSonomy. 2015. Available online: https://www.bibsonomy.org/bibtex/f230a919c34360709aa298734d63dca3 (accessed on 4 March 2022).
39. Love, M.I.; Huber, W.; Anders, S. Moderated estimation of fold change and dispersion for RNA-seq data with DESeq2. *Genome Biol.* **2014**, *15*, 550. [CrossRef] [PubMed]
40. Anders, S.; Huber, W. Differential expression analysis for sequence count data. *Genome Biol.* **2010**, *11*, R106. [CrossRef] [PubMed]
41. Patil, K.R.; Nielsen, J. Uncovering transcriptional regulation of metabolism by using metabolic network topology. *Proc. Natl. Acad. Sci. USA* **2005**, *102*, 2685–2689. [CrossRef] [PubMed]

42. Väremo, L.; Nielsen, J.; Nookaew, I. Enriching the gene set analysis of genome-wide data by incorporating directionality of gene expression and combining statistical hypotheses and methods. *Nucleic Acids Res.* **2013**, *41*, 4378–4391. [CrossRef]
43. Naz, T.; Nosheen, S.; Li, S.; Nazir, Y.; Mustafa, K.; Liu, Q.; Garre, V.; Song, Y. Comparative analysis of beta-carotene production by *Mucor circinelloides* strains CBS 277.49 and WJ11 under light and dark conditions. *Metabolites* **2020**, *10*, 14. [CrossRef] [PubMed]
44. Ratledge, C.; Wynn, J.P. The biochemistry and molecular biology of lipid accumulation in oleaginous microorganisms. *Adv. Appl. Microbiol.* **2002**, *51*, 1–51. [CrossRef] [PubMed]
45. Carsanba, E.; Papanikolaou, S.; Fickers, P.; Erten, H. Screening various *Yarrowia lipolytica* strains for citric acid production. *Yeast* **2019**, *36*, 319–327. [CrossRef]
46. Książek, E. Citric acid: Properties, microbial production, and applications in industries. *Molecules* **2023**, *29*, 22. [CrossRef]
47. Maddox, I.S.; Hossain, M.; Brooks, J.D. The effect of methanol on citric acid production from galactose by Aspergillus niger. *Appl. Microbiol. Biotechnol.* **1986**, *23*, 203–205. [CrossRef]
48. Shaikh, Y.; Jagtap, M.R. Organic acid and solvent production from microbial fermentation. In *Microbial Products for Future Industrialization*; Springer: Berlin/Heidelberg, Germany, 2023; pp. 267–296.
49. Ali, S. Temperature Optima for Citric Acid Accumulation by Aspergillus niger. *Int. J. Biotechnol.* **2002**, *1*, 108–110.
50. Tong, Z.; Zheng, X.; Tong, Y.; Shi, Y.-C.; Sun, J. Systems metabolic engineering for citric acid production by Aspergillus niger in the post-genomic era. *Microb. Cell Factories* **2019**, *18*, 28. [CrossRef] [PubMed]
51. Harris, M.A.; Clark, J.; Ireland, A.; Lomax, J.; Ashburner, M.; Foulger, R.; Eilbeck, K.; Lewis, S.; Marshall, B.; Mungall, C.; et al. The Gene Ontology (GO) database and informatics resource. *Nucleic Acids Res.* **2004**, *32*, D258–D261. [PubMed]
52. Aleksander, S.A.; Balhoff, J.; Carbon, S.; Cherry, J.M.; Drabkin, H.J.; Ebert, D.; Feuermann, M.; Gaudet, P.; Harris, N.L.; Hill, D.P. The Gene Ontology knowledgebase in 2023. *Genetics* **2023**, *224*, iyad031. [CrossRef] [PubMed]
53. Kanehisa, M.; Sato, Y.; Kawashima, M.; Furumichi, M.; Tanabe, M. KEGG as a reference resource for gene and protein annotation. *Nucleic Acids Res.* **2016**, *44*, D457–D462. [CrossRef]
54. Kanehisa, M. Enzyme annotation and metabolic reconstruction using KEGG. In *Protein Function Prediction*; Humana Press: Totowa, NJ, USA, 2017; pp. 135–145.
55. Fazili, A.B.A.; Shah, A.M.; Zan, X.; Naz, T.; Nosheen, S.; Nazir, Y.; Ullah, S.; Zhang, H.; Song, Y. *Mucor circinelloides*: A model organism for oleaginous fungi and its potential applications in bioactive lipid production. *Microb. Cell Factories* **2022**, *21*, 29. [CrossRef]
56. Rodriguez-Martinez, A.; Ayala, R.; Posma, J.M.; Harvey, N.; Jiménez, B.; Sonomura, K.; Sato, T.-A.; Matsuda, F.; Zalloua, P.; Gauguier, D.; et al. pJRES Binning Algorithm (JBA): A new method to facilitate the recovery of metabolic information from pJRES 1H NMR spectra. *Bioinformatics* **2019**, *35*, 1916–1922. [CrossRef] [PubMed]
57. Mehrshad, M.; Salcher, M.M.; Okazaki, Y.; Nakano, S.-I.; Šimek, K.; Andrei, A.-S.; Ghai, R. Hidden in plain sight—Highly abundant and diverse planktonic freshwater Chloroflexi. *Microbiome* **2018**, *6*, 176. [CrossRef]
58. Wang, X.; Han, F.; Yang, M.; Yang, P.; Shen, S. Exploring the response of rice (*Oryza sativa*) leaf to gibberellins: A proteomic strategy. *Rice* **2013**, *6*, 17. [CrossRef] [PubMed]
59. Suparmin, A.; Kato, T.; Takemoto, H.; Park, E.Y. Metabolic comparison of aerial and submerged mycelia formed in the liquid surface culture of *Cordyceps militaris*. *Microbiologyopen* **2019**, *8*, e00836. [CrossRef] [PubMed]
60. Ray, S.K. Modulation of autophagy for neuroprotection and functional recovery in traumatic spinal cord injury. *Neural Regen. Res.* **2020**, *15*, 1601–1612. [CrossRef] [PubMed]
61. Singh, S.; Brocker, C.; Koppaka, V.; Chen, Y.; Jackson, B.C.; Matsumoto, A.; Thompson, D.C.; Vasiliou, V. Aldehyde dehydrogenases in cellular responses to oxidative/electrophilicstress. *Free. Radic. Biol. Med.* **2013**, *56*, 89–101. [CrossRef]
62. Barski, O.A.; Tipparaju, S.M.; Bhatnagar, A. The Aldo-Keto reductase superfamily and its role in drug metabolism and detoxification. *Drug Metab. Rev.* **2008**, *40*, 553–624. [CrossRef]
63. Black, P.N.; DiRusso, C.C. Yeast acyl-CoA synthetases at the crossroads of fatty acid metabolism and regulation. *Biochim. Biophys. Acta (BBA)-Mol. Cell Biol. Lipids* **2007**, *1771*, 286–298. [CrossRef] [PubMed]
64. Zhou, X.; Rao, S.; Wrightstone, E.; Sun, T.; Lui, A.C.W.; Welsch, R.; Li, L. Phytoene synthase: The key rate-limiting enzyme of carotenoid biosynthesis in plants. *Front. Plant Sci.* **2022**, *13*, 884720. [CrossRef] [PubMed]
65. Sonnabend, R.; Seiler, L.; Gressler, M. Regulation of the leucine metabolism in *Mortierella alpina*. *J. Fungi* **2022**, *8*, 196. [CrossRef]
66. Bulfer, S.L.; Scott, E.M.; Couture, J.-F.; Pillus, L.; Trievel, R.C. Crystal structure and functional analysis of homocitrate synthase, an essential enzyme in lysine biosynthesis. *Biophys. J.* **2010**, *98*, 450a. [CrossRef]
67. Fouquerel, E.; Goellner, E.M.; Yu, Z.; Gagne, J.P.; de Moura, M.B.; Feinstein, T.; Wheeler, D.; Redpath, P.; Li, J.; Romero, G.; et al. ARTD1/PARP1 negatively regulates glycolysis by inhibiting hexokinase 1 independent of NAD + Depletion. *Cell Rep.* **2014**, *8*, 1819–1831. [CrossRef] [PubMed]
68. Ham, H.J.; Seo, J.; Yoon, H.-J.; Shin, S.K. Label-free measurement of the yeast short chain TAG lipase activity by ESI-MS after one-step esterification. *J. Lipid Res.* **2017**, *58*, 625–631. [CrossRef] [PubMed]

69. Borrelli, A.; Bonelli, P.; Tuccillo, F.M.; Goldfine, I.D.; Evans, J.L.; Buonaguro, F.M.; Mancini, A. Role of gut microbiota and oxidative stress in the progression of non-alcoholic fatty liver disease to hepatocarcinoma: Current and innovative therapeutic approaches. *Redox Biol.* **2018**, *15*, 467–479. [CrossRef] [PubMed]
70. Fitzgerald, G.; Soro-Arnaiz, I.; De Bock, K. The warburg effect in endothelial cells and its potential as an anti-angiogenic Target in cancer. *Front. Cell Dev. Biol.* **2018**, *6*, 100. [CrossRef]
71. Franco-Cano, A.; Marcos, A.T.; Strauss, J.; Cánovas, D. Evidence for an arginine-dependent route for the synthesis of NO in the model filamentous fungus *Aspergillus nidulans*. *Environ. Microbiol.* **2021**, *23*, 6924–6939. [CrossRef]
72. Jia, Y.; Tomita, T.; Yamauchi, K.; Nishiyama, M.; Palmer, D.R.J. Kinetics and product analysis of the reaction catalysed by recombinant homoaconitase from *Thermus thermophilus*. *Biochem. J.* **2006**, *396*, 479–485. [CrossRef] [PubMed]
73. Fang, W.; Jiang, L.; Zhu, Y.; Yang, S.; Qiu, H.; Cheng, J.; Liang, Q.; Tu, Z.-C.; Ye, C. Methionine restriction constrains lipoylation and activates mitochondria for nitrogenic synthesis of amino acids. *Nat. Commun.* **2023**, *14*, 2504. [CrossRef] [PubMed]
74. Pan, S.; Fan, M.; Liu, Z.; Li, X.; Wang, H. Serine, glycine and one-carbon metabolism in cancer (Review). *Int. J. Oncol.* **2020**, *58*, 158–170. [CrossRef] [PubMed]
75. Vanhove, K.; Graulus, G.-J.; Mesotten, L.; Thomeer, M.; Derveaux, E.; Noben, J.-P.; Guedens, W.; Adriaensens, P. The metabolic landscape of lung cancer: New insights in a disturbed glucose metabolism. *Front. Oncol.* **2019**, *9*, 1215. [CrossRef] [PubMed]
76. Mentch, S.J.; Locasale, J.W. One-carbon metabolism and epigenetics: Understanding the specificity. *Ann. New York Acad. Sci.* **2015**, *1363*, 91–98. [CrossRef]
77. Dong, Y.; Tu, R.; Liu, H.; Qing, G. Regulation of cancer cell metabolism: Oncogenic MYC in the driver's seat. *Signal Transduct. Target. Ther.* **2020**, *5*, 124. [CrossRef]
78. Ngo, B.; Kim, E.; Osorio-Vasquez, V.; Doll, S.; Bustraan, S.; Liang, R.J.; Luengo, A.; Davidson, S.M.; Ali, A.; Ferraro, G.B.; et al. Limited environmental serine and glycine confer brain metastasis sensitivity to PHGDH inhibition. *Cancer Discov.* **2020**, *10*, 1352–1373. [CrossRef] [PubMed]
79. Weickhmann, A.K.; Keller, H.; Wurm, J.P.; Strebitzer, E.; Juen, M.A.; Kremser, J.; Weinberg, Z.; Kreutz, C.; Duchardt-Ferner, E.; Wöhnert, J. The structure of the SAM/SAH-binding riboswitch. *Nucleic Acids Res.* **2019**, *47*, 2654–2665. [CrossRef]
80. Reisch, C.R.; Moran, M.A.; Whitman, W.B. Bacterial Catabolism of Dimethylsulfoniopropionate (DMSP). *Front. Microbiol.* **2011**, *2*, 172. [CrossRef] [PubMed]
81. Zhang, H.; Zhang, L.; Chen, H.; Chen, Y.Q.; Chen, W.; Song, Y.; Ratledge, C. Enhanced lipid accumulation in the yeast Yarrowia lipolytica by over-expression of ATP:citrate lyase from Mus musculus. *J. Biotechnol.* **2014**, *192*, 78–84. [CrossRef]
82. Wang, L.; Chen, W.; Feng, Y.; Ren, Y.; Gu, Z.; Chen, H.; Wang, H.; Thomas, M.J.; Zhang, B.; Berquin, I.M.; et al. Genome characterization of the oleaginous fungus mortierella alpina. *PLoS ONE* **2011**, *6*, e28319. [CrossRef]
83. Osada, K.; Maeda, Y.; Yoshino, T.; Nojima, D.; Bowler, C.; Tanaka, T. Enhanced NADPH production in the pentose phosphate pathway accelerates lipid accumulation in the oleaginous diatom Fistulifera solaris. *Algal Res.* **2017**, *23*, 126–134. [CrossRef]
84. Sun, X.-M.; Xu, Y.-S.; Huang, H. Thraustochytrid cell factories for producing lipid compounds. *Trends Biotechnol.* **2021**, *39*, 648–650. [CrossRef] [PubMed]
85. Udayan, A.; Pandey, A.K.; Sirohi, R.; Sreekumar, N.; Sang, B.-I.; Sim, S.J.; Kim, S.H. Production of microalgae with high lipid content and their potential as sources of nutraceuticals. *Phytochem. Rev.* **2023**, *22*, 833–860. [CrossRef] [PubMed]